This is an open access article published under an ACS AuthorChoice License, which permits copying and redistribution of the article or any adaptations for non-commercial purposes.

THE JOURNAL OF PHYSICAL CHEMISTRY Letters

Perspective

Cite This: J. Phys. Chem. Lett. 2018, 9, 2326−2337

pubs.acs.org/JPCL

Zero-Dimensional Cesium Lead Halides: History, Properties, and Challenges

Quinten A. Akkerman,[†,‡] Ahmed L. Abdelhady,*[,†] and Liberato Manna*[,†]

[†]Nanochemistry Department, Istituto Italiano di Tecnologia, Via Morego 30, 16163 Genova, Italy

[‡]Dipartimento di Chimica e Chimica Industriale, Università degli Studi di Genova, Via Dodecaneso 31, 16146 Genova, Italy

ABSTRACT: Over the past decade, lead halide perovskites (LHPs) have emerged as new promising materials in the fields of photovoltaics and light emission due to their facile syntheses and exciting optical properties. The enthusiasm generated by LHPs has inspired research in perovskite-related materials, including the so-called "zero-dimensional cesium lead halides", which will be the focus of this Perspective. The structure of these materials is formed of disconnected lead halide octahedra that are stabilized by cesium ions. Their optical properties are dominated by optical transitions that are localized within the individual octahedra, hence the title "'zero-dimensional perovskites". Controversial results on their physical properties have recently been reported, and the true nature of their photoluminescence is still unclear. In this Perspective, we will take a close look at these materials, both as nanocrystals and as bulk crystals/thin films, discuss the contrasting opinions on their properties, propose potential applications, and provide an outlook on future experiments.

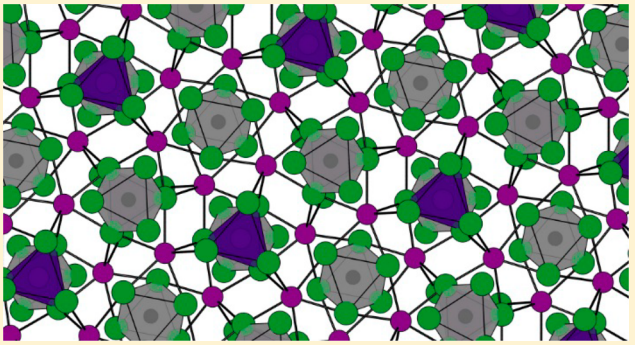

The remarkable properties of lead halide perovskites (LHPs) directly relate to their peculiar crystal structure, the ABX_3 perovskite structure, in which corner-sharing BX_6 octahedra form a cubic framework and A cations fill the voids.[1] The first account of lead halides crystallized in the perovskite structure dates back to 1893, when different colored powders with a $CsPbX_3$ composition, with the color depending on the halide, could be prepared.[2] As was reported in that same work, cesium lead halides can also crystallize as white powders, regardless of the type of halide that is used, with a Cs_4PbX_6 stoichiometry. In this phase, the PbX_6^{4-} octahedra are no longer corner-shared; thus, the photoexcited carriers in these materials experience a much stronger quantum confinement than that of $CsPbX_3$. For this reason, the Cs_4PbX_6 phase is often called a "zero-dimensional (0D) perovskite", although it bears no structural resemblance to the perovskite structure. The Cs_4PbX_6 phase remained almost completely forgotten during the 20th century, with only a few works investigating their optical properties (specifically by Nikl and Kondo et al. during the 1990s and 2000s).[3−9] It was not until 2016 that these Cs_4PbX_6 compounds started to generate interest again, mainly as a result of the surging pursuit in LHPs and related metal halides,[10] and papers began to report Cs_4PbBr_6 powders with strong and stable green photoluminescence (PL).[11,12] Soon after, the first publications on Cs_4PbX_6 nanocrystals (NCs) emerged.[13,14] Interestingly, in stark contrast to the highly emissive $CsPbX_3$ NCs that were first synthesized in 2015[15] and the highly green emitting Cs_4PbBr_6 powders, some of these Cs_4PbX_6 NCs exhibited no PL; instead, they had optical properties that were similar to those described in the first reports on Cs_4PbX_6 in 1893 and in the 1990s.[13] Furthermore, these optical properties were also similar to those of individual $[PbBr_6]^{4-}$ clusters.[16] The proposed origin of the green PL is either intrinsic to Cs_4PbBr_6 (due to the presence of defects)[11,12,14,17−26] or from contamination by $CsPbBr_3$ NC-like impurities.[13,27−42]

> Although the majority of papers on this topic agree that these materials have a large bandgap (>3.2 eV), the origin of the absorption in the visible spectrum and of the green PL that has been reported for various Cs_4PbBr_6 NCs, powders, and single crystals is still under debate.

In this Perspective, we will examine the literature on 0D cesium metal halides, focusing on Cs_4PbX_6, both in their bulk form and as NCs. We will discuss both old and recent literature concerning this phase, and we will compare current attributions to the origin of the strongly downshifted PL. In addition, we will suggest further experiments that, in our opinion, will help

Received: February 22, 2018
Accepted: April 13, 2018
Published: April 13, 2018

© 2018 American Chemical Society

DOI: 10.1021/acs.jpclett.8b00572
J. Phys. Chem. Lett. 2018, 9, 2326−2337

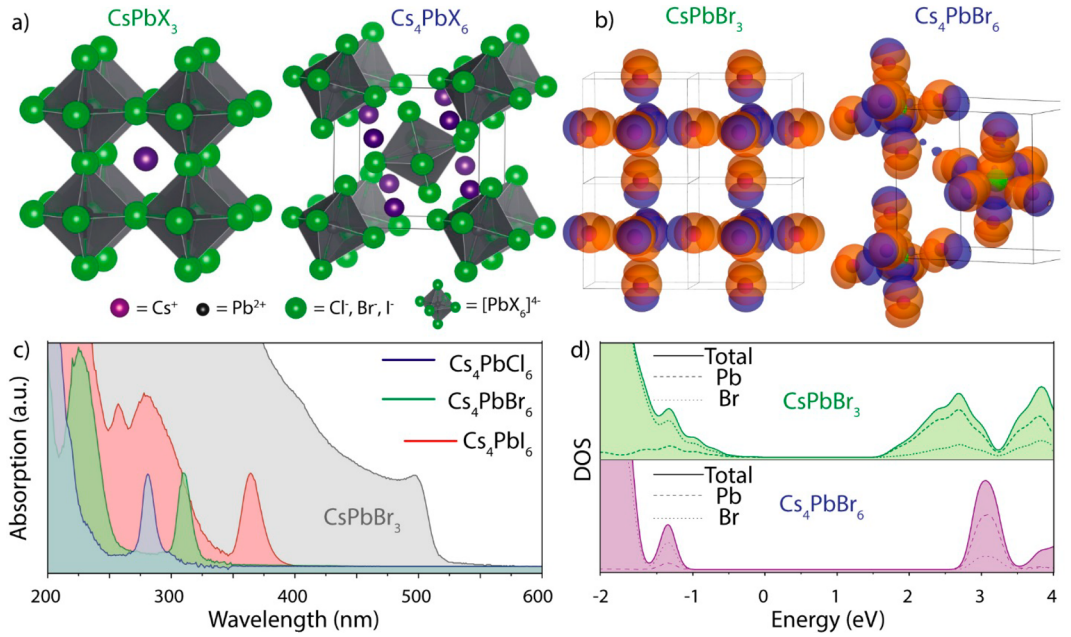

Figure 1. Properties of Cs_4PbX_6 and $CsPbBr_3$. (a) Crystal structures of cubic $CsPbX_3$ and rhombohedral Cs_4PbX_6 (shown in its primitive cubic cell). (b) Comparison of orbital overlap between the p orbitals of each Br^- anion and the s and p orbitals of Pb^{2+} cations, showing the strong orbital overlap of the $[PbBr_6]^{4-}$ clusters in $CsPbBr_3$ and the decoupling in Cs_4PbBr_6, courtesy of Urko Petralanda. (c) Comparison of the absorption spectra of Cs_4PbX_6 and $CsPbBr_3$ NCs, showing the large bandgaps and strong excitonic absorption for Cs_4PbX_6, adapted from ref 13. (d) DFT density of state calculations for $CsPbBr_3$ and Cs_4PbBr_6, adapted from ref 13.

to clarify the optical properties. Finally, we will discuss potential future applications, as well as postsynthesis transformations of Cs_4PbBr_6 NCs into highly luminescent $CsPbBr_3$ NCs.

We start the Perspective with a description of the cubic (3D) LHP crystal structure due to its relation with the Cs_4PbX_6 phase. In this structure, $[PbX_6]^{4-}$ octahedra corner-share each X^- anion between two octahedra, resulting in a cubic (or pseudo-cubic, like orthorhombic/tetragonal, depending on the sizes of the A and X ions) Pb−X−Pb framework,[43] as shown in Figure 1a. To charge balance and provide geometrical stability, the lead halide framework can be stabilized by monovalent cations (often depicted as "A"), which can be in the form of Cs^+, or organic cations like methylammonium (MA) or formamidinium (FA). The rules on whether perovskite structures are stable or not (the so-called Goldschmidt tolerance factor, t) are mainly defined by the ionic radii (r) of A, B, and X and can be determined by using the formula $t = (r_A + r_X)/\sqrt{2(r_B + r_X)}$, with stable perovskites generally forming with $t = 0.7-1$.[1] Long before LHPs became popular in photovoltaics and NC chemistry, it had already been reported that cesium lead halides can crystallize in two other stoichiometries: $CsPb_2X_5$ and Cs_4PbX_6.[2] The Cs_4PbX_6 phase has a crystal structure that is very different from that of $CsPbX_3$; while the $[PbX_6]^{4-}$ octahedra in Cs_4PbX_6 are still surrounded by eight Cs^+ atoms, which is similar to the cubic LHP phase, the halides in Cs_4PbX_6 are no longer shared between $[PbX_6]^{4-}$ octahedra. Furthermore, the Cs^+ atoms in Cs_4PbX_6 are no longer all occupying identical crystallographic sites but actually two distinct sites.[29] Overall, this results in a rhombohedral ($R\bar{3}c$) Cs_4PbX_6 phase, as shown in Figure 1a. An alternative way to perceive Cs_4PbX_6 is to take the cubic $CsPbX_3$ phase and remove 3/4 of the PbX_2 while still maintaining the cubic framework of Cs^+ ions and keeping the remaining PbX in $[PbX_6]^{4-}$ octahedra. Due to the large voids that are created by the removal of PbX_2, the system strongly compresses and distorts, resulting in a Cs_4PbX_6 phase.[29] In contrast to the cubic LHP phase, 0D cesium lead halides seem to be less sensitive to the ratios of the ionic radii of the A, Pb, and X components as a wide variety of A−Pb−X systems can crystallize in the rhombohedral A_4PbX_6 structure (with A = Cs, Rb, K; X = F, Cl, Br, I).[44] This general rhombohedral A_4BX_6 structure is often referred to as the "K_4CdCl_6 structure",[44] and it can be found in a wide range of metal halides (M = Sn, Cd, Mn, Mg, Ca, etc. and with A = (NH_4), Cs, Rb, K,) with a set of formation rules that are similar to those of the Goldschmidt tolerance factor and are based on the ionic B/X and A/X radii.[45] Although it is beyond the scope of this review, the 0D A_4BX_6 crystal structure can even be found in oxides such as Sr_4IrO_6 and Ca_4RuO_6.[46]

Due to the (almost) perfect linear alignment of the Pb^{2+} ions and the halide ions in the LHP framework, the p orbitals of each X^- ion have a good overlap with the s and p orbitals of the two Pb^{2+} atoms with which it is shared (Figure 1b). This orbital overlap leads to a large orbital hybridization, resulting in a marked decrease in the bandgap from a single $[PbX_6]^{4-}$ cluster (about 4 eV in solution for $[PbBr_6]^{4-}$)[16] to $CsPbBr_3$ (about 2.15 eV, bulk). Due to the symmetry of the Cs_4PbX_6 phase, which is lower than the cubic/orthorhombic $CsPbX_3$ phase, one $[PbX_6]^{4-}$ octahedron in Cs_4PbBr_6 has two different $[PbX_6]^{4-}$ octahedra as its nearest neighbors, with Pb−Pb distances of 8.7 and 10 Å, respectively (compared to a 5.9 Å Pb−Pb distance between neighboring $[PbX_6]^{4-}$ octahedra in orthorhombic $CsPbBr_3$).[29] As mentioned above, in Cs_4PbX_6, the $[PbX_6]^{4-}$ octahedra do not share halides; thus, they exhibit negligible orbital overlap between neighboring octahedra, as shown in Figure 1b. As was reported in 1893 alongside with the first works on $CsPbX_3$, Cs_4PbX_6 powders are colorless, independent of the type of halide.[2] Indeed, the reported bandgaps are all in the UV region, with Cs_4PbCl_6 = 4.37 eV, Cs_4PbBr_6 = 3.95 eV, and Cs_4PbI_6 = 3.38 eV, as shown in Figure 1c.[3,6,8,9] The decoupled $[PbX_6]^{4-}$ octahedra in Cs_4PbX_6,

DOI: 10.1021/acs.jpclett.8b00572
J. Phys. Chem. Lett. 2018, 9, 2326−2337

compared to the halide-coupled $[PbX_6]^{4-}$ octahedra in LHP, cause the bandgap of Cs_4PbX_6 to shift toward values of free $[PbX_6]^{4-}$ clusters in solutions and essentially lead to single molecule-like, excitonic absorption bands.[13,16,29] The fact that Cs_4PbX_6 phases have bandgap values close to their respective free $[PbX_6]^{4-}$ clusters is also evident from the optical properties of a series of alkali metal halides (AX, A = Na, K, Rb, Cs; X = Cl, Br, I) doped with Pb^{2+}.[47] For these materials, the spectral position of the excitonic absorption is almost independent of the alkali metal (NaBr:Pb^{2+} = 304 nm, CsBr:Pb^{2+}, = 313 nm Cs_4PbBr_6 = 314 nm),[47,48] while it is strongly dependent on the halide ion. The single-cluster behavior of Pb^{2+} in Cs_4PbBr_6 is also supported by various density functional theory (DFT) calculations, which have confirmed that Cs_4PbX_6 compounds have large bandgaps (Figure 1d).[13,17,19,29,41] That the dimensional reductions of the Pb−X−Pb framework in LHPs have a strong effect on the optical properties is also evident in the lead iodide perovskites. For instance, cubic $CsPbI_3$ is thermally unstable at room temperature, and it undergoes a phase transition to an orthorhombic phase. Here, the lead iodide octahedra are disconnected and reordered into linear chains so that the dimensionality in the interconnection of the $[PbX_6]^{4-}$ octahedra is reduced from 3D to 1D,[49] and an increase in the bandgap from 1.73 to 2.25 eV can be observed. Similarly, cubic $FAPbI_3$ undergoes a transition to a more stable nonperovskite hexagonal phase at low temperatures, with the lead iodide octahedra completely disconnected, resulting in the bandgap being significantly higher than that in the cubic phase.[50] Moreover, 2D Ruddlesden−Popper phases, as well as layered $CsPb_2X_5$, exhibit electronic, absorption, and PL properties that are very different than those of the corresponding LHPs.[51,52]

Despite the wide bandgap of Cs_4PbBr_6, several groups have recently reported strong green PL as well as absorption in the green region of the spectrum from Cs_4PbBr_6 powders, single crystals, and NCs.[11,17,53,54] This green PL from Cs_4PbBr_6 had already been observed in the early 1990s by Nikl et al., who conducted a series of experiments on CsX:Pb^{2+}, Cs_4PbX_6, and $CsPbX_3$, with the aim of studying the optical properties of Pb^{2+} in different cesium halide matrixes.[3−6,55,56] It was noticed that the Cs_4PbBr_6 absorption at around 4 eV often was accompanied by both weak absorption and strong PL in the green region around 2.4 eV (Figure 2a,b). Nikl et al. concluded that "it is difficult to hold back the occurrence of the $CsPbX_3$ (X = Cl, Br) phase completely" and that "the unwanted coexistence of these two phases in the Cs_4PbX_6 crystals most probably arises because of an unavoidable incongruent melting crystal growth process". Kondo et al. performed a similar series of experiments, and also concluded that "Cs_4PbBr_6 crystals usually coexist with the $CsPbBr_3$ and/or CsBr phases."[7−9,57−60] Nikl et al. further studied the coexistence of $CsPbBr_3$ and CsBr, and they hypothesized that the green luminescence that is seen in Pb-doped CsBr single crystals arose most likely from the presence of $CsPbBr_3$ quantum dots.[55] Similarly, $CsPbCl_3$ NC-like clusters with PL and absorption at around 400 nm could be crystallized inside of CsCl, and $CsPbI_3$ (in the yellow δ-phase) impurities were observed in Cs_4PbI_6 and CsI.[4,47] The procedure of embedding perovskite NCs in a halide-based matrix was recently also extended to hybrid organic−inorganic perovskites, in which $MAPbBr_3$ NCs were embedded in a MABr matrix.[61] All of these works indicated that the CsX, Cs_4PbX_6, and $CsPbX_3$ phases are miscible and often coexist, and that the PL originates from small $CsPbX_3$ NC-like impurities (Figure 2c,d).

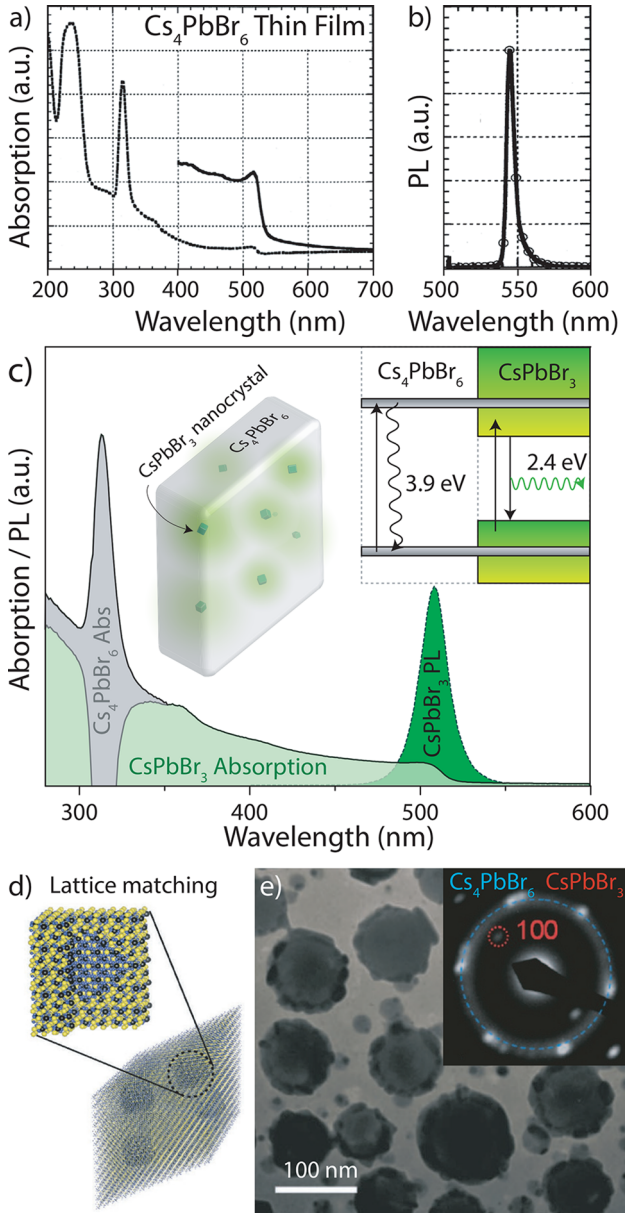

Figure 2. Overview of studies describing the embedment of $CsPbBr_3$ in Cs_4PbBr_6. (a) Cs_4PbBr_6 thin films exhibiting appreciable absorption at around 520 nm, (b) accompanied by narrow PL at 550 nm originating from the presence of $CsPbBr_3$. Adapted from ref 6. (c) Schematic representation of a band structure and absorption/PL spectrum of $CsPbBr_3$ NCs embedded in a Cs_4PbBr_6 matrix. The absorption spectrum exhibits strong excitonic absorption at around 315 nm due to the Cs_4PbBr_6 host and broad absorption up to 515 nm due to the absorption of the $CsPbBr_3$ NCs, which emit at the band edge (around 515 nm). (d) Theoretical model for a $Cs_4PbBr_6|CsPbBr_3$ composite material, with various embedded cubic $CsPbBr_3$ NCs in a rhombic Cs_4PbBr_6 prism matrix, adapted from ref 62. (e) TEM image and electron diffractogram of a $Cs_4PbBr_6|CsPbBr_3$ composite, indicating the existence of small $CsPbBr_3$ NCs in the Cs_4PbBr_6 host, adapted from ref 30.

More recently, small $CsPbBr_3$ NCs encapsulated in a Cs_4PbBr_6 matrix were found to have high PL quantum yields (PLQYs) and were used to fabricate temperature-insensitive frequency-upconverted lasers, as was proven by HRTEM.[32,62] Xu et al. proposed a type-I heterostructure for such a system, and they prepared a light-emitting diode (LED) in which the

DOI: 10.1021/acs.jpclett.8b00572
J. Phys. Chem. Lett. 2018, 9, 2326−2337

carriers from the Cs_4PbBr_6 host were injected into the $CsPbBr_3$ NCs.[30] In addition, another LED based on silica encapsulation of the Cs_4PbBr_6-passsivated $CsPbBr_3$ NCs was also reported.[38] Moreover, several groups have used transmission electron microscopy (TEM) to identify the presence of green luminescent $CsPbBr_3$ NCs in Cs_4PbBr_6 microcrystals, as well as in Cs_4PbBr_6 NC solutions (Figure 2e).[30,31,34,62]

Although all of these accounts point toward the coexistence of $CsPbX_3$ aggregates in CsX and Cs_4PbX_6, more recent literature has proposed alternative reasons for the green PL in Cs_4PbX_6. These recent works start with the assumption that there is no clear evidence that $CsPbX_3$ is present as the X-ray diffraction (XRD) patterns of Cs_4PbBr_6 show no peaks that are ascribable to $CsPbBr_3$ and elemental analysis yields Cs:Pb:X ratios much closer to 4:1:6 than 1:1:3.[11,12,17,21,35,53] Many of these works provide an alternative explanation for the origin of green PL and absorption, namely, the presence of structural defects in Cs_4PbBr_6, which have been previously reported to strongly influence the PL in 3D and 2D (layered) perovskites.[17,29,63,64] De Bastiani et al. proposed that in Cs_4PbBr_6 the luminescence originates from the presence of bromide vacancies (V_{Br}), which form shallow or deep trap states within the bandgap (Figure 3a,b).[21] Feng et al. proposed another type of defect, which arises from the incorporation of −OH (hydroxide) groups into Cs_4PbBr_6.[29] Through DFT calculations, they indicated that the incorporation of −OH can form a 2.6 eV sub-bandgap state in Cs_4PbBr_6. Recombination from midbandgap states due to crystal defects was also hypothesized as being the origin of the green PL in Cs_4PbBr_6 microdisks.[20]

> While the formation of defect states is a plausible explanation for the existence of intrinsic green PL in Cs_4PbBr_6, it is not in agreement with the current view of the effect of defects in perovskites.

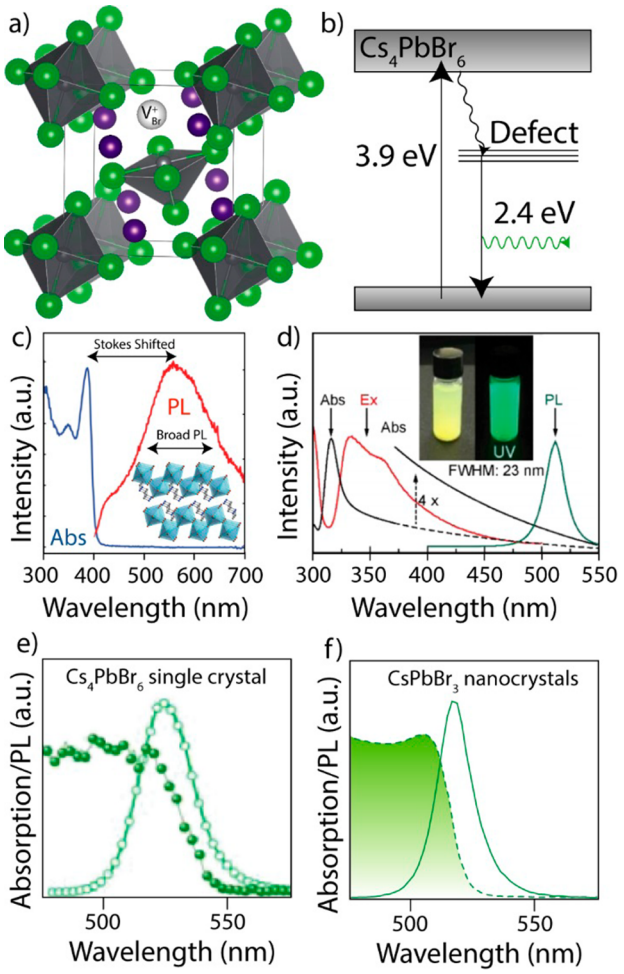

Figure 3. Overview of proposed defect emission in Cs_4PbBr_6. (a) Sketch of a bromide vacancy in Cs_4PbBr_6. (b) Schematic representation of a band structure with a midbandgap defect state, causing midbandgap emission. (c) Defect-related PL emission in a layered 2D organic lead bromide (*N*1-methylethane-1,2-diammonium)$PbBr_4$, adapted from ref 98. (d) Absorption, PL, and PLE from green-emitting 26 nm Cs_4PbBr_6 NCs, showing a narrow PL fwhm and strong quenching of the PL at around 315 nm, adapted from ref 14. (e) Absorption and PL of a green-emitting Cs_4PbBr_6 single crystal, showing narrow band-edge-like PL, adapted from ref 21. (f) Absorption and PL from $CsPbBr_3$ NCs, exhibiting very similar PL and absorption, with narrow PL and a small Stokes shift, adapted from ref 13.

While the formation of defect states is a plausible explanation for the existence of intrinsic green PL in Cs_4PbBr_6, it is not in agreement with the current view of the effect of defects in perovskites. The hypothesis of V_{Br} as a luminescent center is mainly based on the halogen vacancies being the most prominent type of defect in LHPs that are synthesized under halogen-poor conditions. In halide-based materials, halogen vacancies are generally considered as deep traps, and this, in addition to other factors such as the high hole effective mass, accounts for their low carrier transport properties.[65] On the other hand, in LHPs, deep traps often have rather high formation energies and are not easily formed, and most shallow trap states that are formed often do not strongly effect on the optical properties.[66−68] Therefore, LHPs are often described as "defect-tolerant" materials.[43,66−69] For instance, the superior properties of $MAPbI_3$ arise from the absence of deep traps, and iodine vacancies (V_I) only form shallow traps.[66−68,70−74] Similarly, in its bromide counterpart, V_{Br} are generally described as shallow defects.[71] However, V_{Br} and chlorine vacancies (V_{Cl}) in the cubic $MAPbX_3$ (X = Cl, Br) are significantly deeper traps than V_I in the tetragonal $MAPbI_3$.[72] In the case of bromide perovskites, it was concluded that high V_{Br} concentrations result in a lower radiative recombination efficiency and a consequent decrease in PLQY.[75] In the case of $CsPbBr_3$, using a small excess of CsBr precursor (compared to $PbBr_2$) results in decreased V_{Br} concentration and, thus, an enhanced PLQY.[76] The different nature of halide vacancies in perovskites is also evident in lead-free $Cs_2AgInBr_6$ and $Cs_2TlBiBr_6$ double perovskites (elpasolites), where halide vacancies have been reported both as shallow ($Cs_2AgInBr_6$) and deep ($Cs_2TlBiBr_6$), respectively.[77,78] Furthermore, deep traps and midbandgap states in LHPs are often considered band-to-band PL quenchers.[64,79] Emissive midbandgap states are sometimes observed in LHPs, but only under vacuum, and the observed PL in these cases is weak, broad, and Stokes shifted.[64] Thus, it is evident that the nature of the halogen vacancies strongly depends on the crystal structure and the chemical nature of the B cation.[65] Hence, the marked difference in the crystal structures of $CsPbBr_3$ and Cs_4PbBr_6 raises the question: are defects, in particular, V_{Br}, in $CsPbBr_3$ and

DOI: 10.1021/acs.jpclett.8b00572
J. Phys. Chem. Lett. 2018, 9, 2326−2337

Cs_4PbBr_6, of a similar nature? Proper calculations on the effect of defects in Cs_4PbX_6 are still lacking, and drawing parallels between halide vacancies in $CsPbX_3$ and Cs_4PbX_6 should be done with caution. Also, due to the rather different types of bonding of the halides in Cs_4PbX_6, the formation energy of a V_X is likely very different than that in $CsPbX_3$. For instance, unlike $CsPbBr_3$ and its hybrid perovskite counterpart, which are usually found to be bromine-deficient,[80−83] Cs_4PbBr_6 is often reported to have a Br:Pb ratio that is usually higher than 6, thus implying that Cs_4PbBr_6 are rather halide rich.[14,18,20,80] One could therefore expect a rather low density of V_{Br}.

Although it is difficult to experimentally prove or disprove the existence of vacancy-based trap emission in Cs_4PbX_6, one can observe several PL and absorption features in luminescent Cs_4PbBr_6 and compare these with defect emissions in other LHPs. For instance, several marked differences between the reported green PL in an "allegedly" pure 0D Cs_4PbBr_6 and that of a general trap and defect emission in both 2D and 1D organic lead halides, which consist of either layered PbX_6^{4-} clusters (2D) or linear PbX_6^{4-} chains (1D), can be seen in the full with at half-maximum (fwhm) and in the Stokes shift of the PL. In the 2D and 1D systems, the defect emissions exhibit a broad PL, often with fwhms larger than 100−200 nm, which is attributed to efficient exciton self-trapping that acts as an excited-state defect instead of a permanent defect (Figure 3c).[84,85] Examples of 2D and 1D organic lead halide materials exhibiting a Stokes-shifted and broad PL include (EDBE)-[$PbBr_4$] (EDBE = 2,2′-(ethylenedioxy)bis(ethylammonium)) and $C_4N_2H_{14}PbBr_4$.[84,85] Another class of materials with a broad and Stokes-shifted PL are 0D (and also 1D) organic−inorganic Sn^{2+} bromides such as $(C_4N_2H_{14}X)_4SnX_6$ (X = Br or I).[85−87] In these 0D materials, the large organic cations completely isolate each SnX_6^{4-} octahedron. Thus, these materials are considered to exhibit the intrinsic properties of the individual SnX_6^{4-} clusters, and the photoluminescent properties are explained to be not as a result of lattice defects but rather due to excited-state structural reorganization within individual SnX_6^{4-} clusters. This results in them having a long lifetime, in the range of a few microseconds. Hence, Zhou et al. concluded that the SnX_6^{4-} octahedra could be thought of as either "crystal lattice points" or "molecular species".[87] In stark contrast with the optical behavior of these compounds, the green PL in Cs_4PbBr_6 is often reported to have a very narrow fwhm (15−25 nm), as is shown in Figure 3d,e.[12,18,21] This narrow PL matches that of $CsPbX_3$ NCs (12−42 nm, Figure 3f), and that of the first accounts for $CsPbBr_3$ NCs embedded in CsBr (0.11 eV, compared to 0.12 eV for colloidal 8 nm $CsPbBr_3$ NCs).[15,56,88] It is also similar to other confined NCs with band-edge PL.[89] As mentioned above, the defect emission in a LHP is often observed with a large Stokes shift as defect states are formed midbandgap (Figure 3b,c).

Although the green PL in Cs_4PbBr_6 is sometimes referred to as being Stokes-shifted or as having down-shifted PL (originating from the 3.9 eV bandgap of Cs_4PbBr_6), almost all green luminescent Cs_4PbBr_6 nano/micro/bulk crystals clearly also absorb strongly in the green region (this can be simply deduced by their green/yellow color, Figure 3d,e).[11,18,21,90] If the green PL were to originate from a midgap state or a trap state, then the absorption of the Cs_4PbBr_6 host would remain unaltered, i.e., it would have no features in the visible range. Take, for example, the case of fluorescent, low-dimensional organic−inorganic lead or tin halides,[85,91−94] in which the dimensionality (whether 2D, 1D, or 0D) is tuned by using specially designed amines, like 2,2′-(ethylenedioxy)bis-(ethylamine), $C_4N_2H_{14}^{2+}$, or $C_4N_2H_{14}Br^+$. In all of these low-dimensional organic lead and tin halides, the strong dimensional confinement results in large bandgaps in the ultraviolet region of the spectrum, and powders of all of these materials are, indeed, white in color. These lower-dimensional organic lead and tin halides can also exhibit down-converted (100−200 nm) emission in the visible spectrum, and their PL excitation (PLE) matches their absorption spectra.[86,87] In the case of the green luminescent Cs_4PbBr_6, the absorption and PLE spectra show features in the visible range (around 510−520 nm), which is in the same range as the green PL. The green PL in the Cs_4PbBr_6 is therefore often reported with a very small Stokes shift of only 28 meV,[11,21] suggesting that the green PL originates from a direct band−band transition in the visible, rather than from emission from a midgap defect state (Figure 3e). Additionally, the PLE spectra from allegedly "pure" Cs_4PbBr_6 and from samples of $CsPbBr_3$ encased in a Cs_4PbBr_6 matrix are identical.[32] In both cases, strong absorption at visible wavelengths along with a sharp absorption decrease (with most cases having no absorption at all) at shorter wavelengths (315 nm) are observed (Figure 3d). This can be explained by the presence of two band edges that correspond to two different materials (Figure 2b). Furthermore, the green PL reported for the "pure" 0D phase was actually completely quenched when excited at the bandgap of Cs_4PbBr_6 (at around 4 eV).[11] In the work by Wang et al., in which they reported $CsPbBr_3$ NCs in a Cs_4PbBr_6 matrix, excitation at around 4 eV resulted in a dwindled green emission, and the spectrum was instead dominated by broad ultraviolet emission (~370 nm).[32] This again indicates that the green PL does not originate from Cs_4PbBr_6 but rather from a lower-bandgap material ($CsPbBr_3$). In addition, in thin films of $CsPbBr_3|Cs_4PbBr_6$ composites, the intensity of the absorption in the green region decreases as the concentration of $CsPbBr_3$ is reduced.[40] This observation might explain the absence of an absorption peak in the visible range for the small (26 nm) green-emitting Cs_4PbBr_6, for which only an absorption tail is recorded.[14] To our knowledge, no explanation has been given for the absorption in the green region for supposedly pure Cs_4PbBr_6.

Although the green PL in Cs_4PbBr_6 can indeed be explained by the presence of small $CsPbBr_3$ NCs, there are still a few observations that require further scrutiny.

The aforementioned defect emission properties (i.e., the large Stokes shift and large fwhm) are also observed in different binary and ternary chalcogenide quantum dots. For instance, selenium vacancies in CdSe NCs give rise to a broad and Stokes-shifted deep trapped emission, and a higher defect emission is observed for smaller NCs due to their larger surface/volume ratio.[95] Doping chalcogenide NCs can also cause defect emission; a typical example of this can be seen in Ag-doped CdSe NCs, which manifest enhanced band-edge emission compared to the undoped NCs. However, these Ag-doped CdSe NCs also show broad, Stokes-shifted emission, which is attributed to defect emission.[96] Another example is the donor−acceptor defect emission in highly emissive $CuInS_2$

DOI: 10.1021/acs.jpclett.8b00572
J. Phys. Chem. Lett. 2018, 9, 2326−2337

NCs, which is characterized by a large Stokes shift and PL fwhm of about 100 nm.[97]

In addition to the directly observable green PL and absorption, several other optical measurements on green luminescent Cs_4PbBr_6 raise questions about its origins. Recent transient absorption measurements on green luminescent Cs_4PbBr_6 films by Yin et al.[19] were interpreted by assuming a short polaron lifetime of ~2 ps, and the hypothesis of polaronic features in Cs_4PbBr_6 was confirmed by other groups.[41] However, the transient absorption data strongly resemble those of colloidal $CsPbBr_3$ NCs, as was reported by Wu et al.[99] In both the works of Yin et al. and Wu et al., at fast delay times (0.2−0.5 ps), an exciton bleach was observed at the lowest-energy excitonic band, and an exciton absorption feature was observed 15 nm above the band edge. Moreover, in both the green luminescent Cs_4PbBr_6 films of Yin et al. and the $CsPbBr_3$ NCs of Wu et al., the exciton-induced shift almost completely disappeared after 2 ps, and the TA spectra only exhibited exciton bleach at the bandgap. Because Yin et al. did not consider the possibility of inclusions of $CsPbBr_3$ NCs in their model and they did not compare their results with Wu et al.'s data, it would be interesting to reanalyze the TA measurements taking the consideration of $CsPbBr_3$ NC-like impurities in mind.

The uncertainty regarding the optical properties of the green-emitting pure Cs_4PbBr_6 extends to PL lifetimes. Here, again, the short PL lifetimes of the green PL from Cs_4PbBr_6 are very similar to those of $CsPbBr_3$ NCs.[11,21,30,53] For instance, in the work on Cs_4PbBr_6 single crystals, De Bastiani et al. concluded that "This PL lifetime is closer to the lifetime of perovskite-quantum dots (QD) than usual perovskite single crystals."[21] Similarly, Saidaminov et al. reported a PL lifetime of Cs_4PbBr_6 powders that is 2 orders of magnitude faster than that of the LHP single crystals.[11] On the other hand, results by Cha et al. disagree with the above reports as they measured average PL lifetimes of 19.58 and 2.43 ns for Cs_4PbBr_6 and $CsPbBr_3$ single crystals, respectively.[53] Ling et al. found that the PL lifetime of their $CsPbBr_3|Cs_4PbBr_6$ composite increased as the Cs_4PbBr_6 ratio increased.[40] In the case of Cs_4PbBr_6 microdisks, an average PL lifetime of 11.95 ns was recorded at the center of the disks only,[20] whereas a shorter PL lifetime (9.26 ns) was recorded at the disks' edges, indicating that there is a spatial inhomogeneity within the disks. Generally, PL lifetimes of the bulk (single crystals and powders) green-emitting Cs_4PbBr_6, in most reports discussed above and others, are in agreement with PL lifetimes of $CsPbBr_3$ NCs, suggesting that the high PLQY is due to Cs_4PbBr_6-passivated $CsPbBr_3$ NCs.[12,62]

One final interesting observation is with regard to annealing luminescent Cs_4PbBr_6 single crystals. De Bastiani et al. observed that through annealing aggregates of $CsPbBr_3$ NCs were formed within the single crystals. It was observed that annealing above 250 °C results in the formation of 10 nm sized $CsPbBr_3$ NCs (as determined by XRD).[21] This was explained as triggered by the V_{Br} defects in Cs_4PbBr_6 samples, which act as "initialization centers". Although the PLQYs of 10 nm $CsPbBr_3$ NCs is often found to be in the range of 80−95%,[15,100] it was reported that the formed $CsPbBr_3$ NCs within the single crystal actually strongly quenches the PL. This is rather contradictory as one would expect an increase in the PLQY when $CsPbBr_3$ NCs are formed.

As mentioned earlier, the argument that is generally used to prove that the green emission is an intrinsic property of Cs_4PbBr_6 is the lack of $CsPbBr_3$ diffraction peaks. For instance, no $CsPbBr_3$ diffractions peaks were reported in various Cs_4PbBr_6 samples, including powders, single crystals, and NCs.[11,14,17,18,20,21] For instance, De Bastiani et al. were able to demonstrate that the presence of any $CsPbBr_3$ impurity phase down to 0.5% in weight could be detected by XRD (Figure 4a).[21] Nevertheless a similar experiment, in which non-

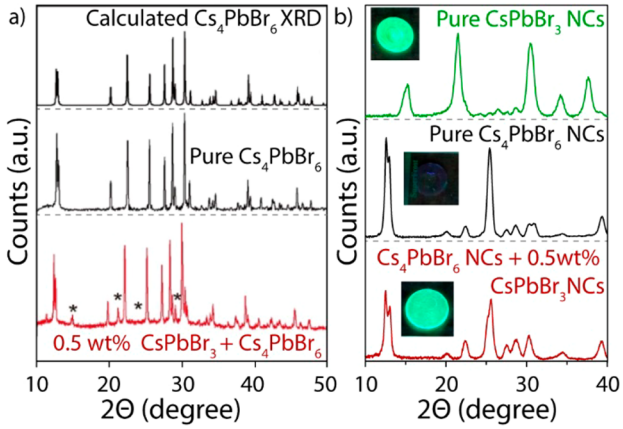

Figure 4. XRD data. (a) XRD calibration experiment indicating that the synthesized Cs_4PbBr_6 single crystals were either pure or contained less than 0.5 wt % of $CsPbBr_3$, adapted from ref 21. (b) Similar experiment performed with NCs, in which Cs_4PbBr_6 NCs were mixed (2% molar, 0.5 wt %) with $CsPbBr_3$ NCs, indicating strong green PL after mixing but no detectable $CsPbBr_3$ XRD diffraction peaks.

luminescent Cs_4PbBr_6 NCs were mixed with a small amount (2% molar, 0.5 wt %) of highly luminescent $CsPbBr_3$ NCs, indicated that this small amount of $CsPbBr_3$ did not result in any clear $CsPbBr_3$ features in the XRD pattern (Figure 4b).[13] Furthermore, XRD patterns of $Cs_4PbBr_6|CsPbBr_3$ composites also indicated that there were not any detectable $CsPbBr_3$ XRD diffractions.[40,62] This is expected as diffractions from $CsPbBr_3$ NCs should be extremely low in intensity, not only due to their low concentration but also due to the very broad and low-intensity diffraction peaks of NCs. This is clear from the XRD patterns of borosilicate glasses doped with 4 nm $CsPbX_3$ NCs, which hardly exhibit any perovskite XRD peaks even though the glasses are strongly absorbent and brightly luminescent, indicating that there is a high concentration of NCs.[101]

One additional open question is whether the high PLQY in $Cs_4PbBr_6|CsPbBr_3$ composites is due only to the formation of $CsPbBr_3$ NCs or whether it also arises from a synergistic effect at the $CsPbBr_3|Cs_4PBr_6$ interface.

Thus, it is very tempting to suggest that the optical properties of the green-emitting Cs_4PbBr_6 originates from $CsPbBr_3$ NC impurities because they have similar PLs and absorptions, PLQYs, and lifetimes. One more synthetic clue toward the formation of $CsPbBr_3$ NCs inside of bulk Cs_4PbBr_6 is derived from the results of the synthesis of nonluminescent Cs_4PbX_6 NCs.[13,33,37,102] These Cs_4PbX_6 NCs exhibit no PL and no absorption in the visible region, with only strong excitonic absorption in the UV, and can be synthesized in the 10−100

DOI: 10.1021/acs.jpclett.8b00572
J. Phys. Chem. Lett. 2018, 9, 2326−2337

nm size range. These Cs_4PbX_6 NCs are spherical or hexagonally shaped for small NCs (<20 nm) and often rhombohedral for larger NCs, which strongly differs from the highly cubic $CsPbX_3$ NCs, and strongly reflects their hexagonal crystal structure.[13,33,37] Interestingly, these NCs are often synthesized under similar conditions to those of the highly luminescent $CsPbBr_3$ NCs, but they use a higher amount of alkylamine. Here, the nucleation of $CsPbBr_3$ can be completely suppressed because oleylamine strongly binds to Pb^{2+}.[33,37,102] Even though these NCs are synthesized under stoichiometric conditions closer to $CsPbBr_3$ (Cs:Pb:Br = 2.2:1:2),[13] only the Cs_4PbBr_6 phase was formed; therefore, no green PL was observed. This would then explain how both green luminescent and nonluminescent Cs_4PbBr_6 NCs could be synthesized by the simple addition of more ligands; the increased ligand amount suppresses the formation of $CsPbBr_3$.[17] The Cs_4PbX_6 NCs were also the first to be reported with mixed halide compositions, as confirmed with both absorption and XRD.[13,37] These mixed halide Cs_4PbX_6 NCs exhibit rather broadening of their exitonic absorption compared with the single halide Cs_4PbX_6 NCs. The broadening of the absorption is a direct result of the individual decoupled, mixed halide $[PbBr_nX_{6-n}]^{4-}$ clusters, which can only be populated with integer n = 0, 1, 2, up to 6, resulting in broad absorption due to the contributions of different $[PbBr_nX_{6-n}]^{4-}$ octahedra within the NC.[13]

Although the green PL in Cs_4PbBr_6 can indeed be explained by the presence of small $CsPbBr_3$ NCs, there are still a few observations that require further scrutiny. One striking and consistent feature of the green PL in the reported luminescent Cs_4PbBr_6 is its peak position. For many Cs_4PbBr_6 single crystals, powders, and NCs, the PL is always found in a rather narrow range, from 515 to 524 nm. Although this is coincidentally in the same range as for 8−15 nm sized $CsPbBr_3$ NCs, it would mean that the formed $CsPbBr_3$ NCs would always be in the same range of sizes and would never be formed with a size smaller than ∼5 nm as this would result in blue-shifted PL due to the quantum confinement effects on $CsPbBr_3$. However, our group has recently demonstrated that the size of the formed $CsPbBr_3$ NCs is highly dependent on the synthetic procedure, including synthesis temperature and ligand ratios.[102] Blue-emitting Cs_4PbBr_6 composites were only very recently reported by Chen et al., who were able to synthesize both blue- and green-emerging Cs_4PbBr_6 cm-sized single crystals embedded with $CsPbBr_3$ NCs.[34] Here, it was observed that during the crystallization first small blue-emitting NCs were formed. Interestingly, it was reported the blue PL slowly shifted toward the green, even if the single crystals were isolated from their growth media, thus indicating that small blue-emitting $CsPbBr_3$ NCs are thermodynamically less stable than the larger green-emitting $CsPbBr_3$ NCs. Although it was speculated that the $CsPbBr_3$ NCs were formed due to Pb^{2+} vacancies,[34] a deep study of the formation and growth of these embedded $CsPbBr_3$ NCs is still lacking.

One additional open question is whether the high PLQY in $Cs_4PbBr_6|CsPbBr_3$ composites is due only to the formation of $CsPbBr_3$ NCs or whether it also arises from a synergistic effect at the $CsPbBr_3|Cs_4PBr_6$ interface. Quan et al. proposed that the lattice matching at the $CsPbBr_3|Cs_4PBr_6$ interface improves the surface passivation of $CsPbBr_3$ NCs.[62] Ling et al. suggested, however, that the shallow traps that are generated at the $CsPbBr_3|Cs_4PbBr_6$ interface cause an enhancement in the PL.[40] Furthermore, Xu et al. suggested that the change in dielectric constant from the $CsPbBr_3$ NCs to the Cs_4PbBr_6 host could result in an increase of the oscillator strength of the excitons in the imbedded nanocrystal, which increases the radiative decay.[30] It is vital, therefore, to understand whether the $CsPbBr_3|Cs_4PbBr_6$ interface further enhances the PL properties of the $CsPbBr_3$ NCs or not as this might lead to a better understanding of the requirements for encapsulating $CsPbBr_3$ NCs in other materials while maintaining high and stable PLQYs. Finally, it is interesting to note that the $CsPb_2Br_5$ phase, which is a layered 2D structure, is currently facing the same green PL discussion as Cs_4PbBr_6. Various different optical properties have been reported, ranging from a nonluminescent wide indirect bandgap material[52,103−105] to a green material with strong green PL (again, around 515 nm).[22,106−109]

As a result of the stable and high PLQYs, $Cs_4PbX_6|CsPbBr_3$ materials are still interesting for down-converting applications like down-conversion LEDs.

Cs_4PbX_6 phases also exhibit very different electronic properties from $CsPbX_3$ due to their marked structural difference from $CsPbX_3$. In contrast to the highly conductive perovskite phase of $CsPbX_3$,[110] the decoupling of the PbX_6^{4-} octahedra in Cs_4PbX_6 and the large increase in distance between these octahedra carriers strongly confine the carriers to the single octahedra, meaning that Cs_4PbX_6 NCs essentially act as insulators.[53,111] A similar argument stands for Cs_4SnBr_6, which has the same crystal structure as Cs_4PbBr_6. This material was reported to have an electrical conductivity that is more than 200 times lower than that of $CsSnBr_3$.[111] A single crystal of Cs_4PbBr_6 was found to have ultralow photoconductivity (on the order of nA).[53] One work did use the luminescent Cs_4PbBr_6 (reported as a $CsPbBr_3|Cs_4PbBr_6$ composite, with a PLQY of 30%) for an LED.[30] The composites showed an increase in the external quantum efficiency (EQE) compared to that of $CsPbBr_3$, presumably due to the increase in the PLQY; the achieved maximum EQE was only 10^{-3}%, which is several orders of magnitude lower than that of LEDs using $CsPbBr_3$ NCs. This demonstrates that, even though $CsPbBr_3|Cs_4PbBr_6$ composites have a high PLQY, their lack of conductivity hinders their use in LEDs. On the other hand, Tong et al. recently demonstrated that the addition of Cs_4PbBr_6 to a $MAPbI_3|CsPbBr_3$ photodector led to increased and faster deep ultraviolet detection.[42] However, it is important that the electronic and photoconductivity are first properly characterized, before Cs_4PbX_6 can be considered as an interesting material for electron injected applications such as LEDs and photodetectors. One recent work by Yin et al. indeed confirmed that "intrinsic large bandgap, heavy charge carriers, and low electrical conductivity of 0D perovskites limit their application in photovoltaic devices."[19]

As a result of the stable and high PLQYs, $Cs_4PbX_6|CsPbBr_3$ materials are still interesting for down-converting applications like down-conversion LEDs, in which the emissions of the material are achieved via excitation with a blue LED. To this end, there have been only very few publications that have reported proper devices.[32,34] For instance, Chen et al. recently combined a highly luminescent $Cs_4PbBr_6|CsPbBr_3$ single crystal with a $K_2SiF_6:Mn^{4+}$ phosphor as a red emitter and a blue-

DOI: 10.1021/acs.jpclett.8b00572
J. Phys. Chem. Lett. 2018, 9, 2326−2337

emitting GaN chip to create high-quality white light with luminous efficiency of ~151 lm W^{-1} and color gamut of 90.6% Rec. 2020 at 20 mA, which was reported to be "much better than that based on conventional perovskite nanocrystals." Furthermore, Wang et al. demonstrated that the Cs_4PbX_6|$CsPbBr_3$ composites exhibited a temperature-insensitive gain, and they used this for a vertical cavity surface emitting laser, which could operate at temperatures as high as 100 °C.[32] One other problem with having Cs_4PbX_6 as the host material for $CsPbX_3$ is the toxicity of the Cs_4PbX_6. If the active luminescent $CsPbBr_3$ is only several wt %, or even less, the majority of the host (Cs_4PbBr_6) will be inactive. Consequently, this would strongly limit the use of these materials in applications due to the Pb^{2+} toxicity. One alternative could be to find new synthesis approaches that are similar to those used for CsBr|$CsPbBr_3$ composites. These types of alkali metal matrixes, as discussed earlier, were already used in the 1990s in the first reports of $CsPbBr_3$ quantum dots, which were imbedded in CsBr, and were also recently used for organic MABr|$MAPbBr_3$ composites.[55,56,61,112] Although others concluded that traces of CsBr in Cs_4PbBr_6|$CsPbBr_3$ quenched the PL,[40] it would be of great interest to revive these types of host materials for $CsPbBr_3$ as it would significantly lower the required amount of lead. Recently, presynthesized $CsPbX_3$ NCs were, for instance, embedded in potassium halide salts, and they exhibited high PLQYs and long-term stability, which demonstrates the advantage of embedding LHP NCs in other halide-based salts.[113] Novel synthesis approaches for pure CsX NCs have recently been reported and could aid in designing synthesis routes toward CsBr|$CsPbBr_3$ composites.[114] Furthermore, devices have so far been limited to Cs_4PbBr_6|$CsPbBr_3$, and it remains to be seen whether or not other halide-based composites, like Cs_4PbI_6|$CsPbI_3$, are stable enough to use in devices.

Although Cs_4PbX_6|$CsPbX_3$ composites exhibit a low potential for applications, Cs_4PbX_6 NCs can be transformed into $CsPbBr_3$ NCs by various reactions (Figure 5).[13,27] This can be done via the insertion of $PbBr_2$, the extraction of CsBr with water or with Prussian Blue, or the extraction of Pb^{2+} with amines.[13,27,28,33,37] Several groups have reported that the size and shape of the starting Cs_4PbBr_6 NCs can be used to tune the size of the final $CsPbBr_3$ NCs (Figure 5b).[13,27,28,33,37] The transformed $CsPbBr_3$ NCs exhibit a strong green PL, similar to the PL of directly synthesized $CsPbBr_3$ NCs, and they show no excitonic absorption in the UV from their parent Cs_4PbBr_6 NCs (Figure 5c). Similarly, no Cs_4PbBr_6 diffractions are observed in XRD analyses after the transformation (Figure 5d). Interestingly, the formed $CsPbBr_3$ NCs can be transformed back into Cs_4PbBr_6 NCs via the addition of oleic acid (Figure 5c,d).[33] One interesting advantage of using this pathway to make $CsPbX_3$ NCs is that the Cs_4PbX_6 NCs can be synthesized with a large tunability over their size (from about 10 up to 50 nm), while remaining nearly monodisperse. The narrow size distribution of the Cs_4PbBr_6 NCs can be used to make large (20−50 nm), monodisperse $CsPbBr_3$ NCs, which currently still remains a challenge to overcome by direct $CsPbBr_3$ NC syntheses. Finally, Hu et al. have used a Cs_4PbBr_6 to $CsPbBr_3$ exchange reaction (via the extraction of Cs^+ with water) to synthesis the $CsPbX_3$|SiO_2 and $CsPbBr_3$|Ta_2O_5 Janus NCs,[36] which are among the first examples of colloidal LHP NC heterostructures.

Due to the insulator bandgap and the very low conductive properties of Cs_4PbX_6 (either luminescent or nonluminescent), its widespread use in applications remains to be seen. On the bright side, the field of zero-dimensional perovskites gives us inside knowledge on how to synthesize and stabilize $CsPbX_3$ NCs, without the aid of large, bulky, nonconductive ligands, directly into powders and single crystals, which still remains challenging with regard to colloidally synthesized $CsPbX_3$. While defects such bromine vacancies are proposed as being the origin of the green PL, additional calculations and optical studies will be required to assess the nature of defects in Cs_4PbBr_6 and of radiative decay mechanisms. Also, more extensive studies will have to correlate the properties of Cs_4PbBr_6 with those of other all-inorganic 0D phases, such as, for example, $CsPb_2Br_5$, Cs_2SnX_6, and $Cs_3Bi_2I_9$.

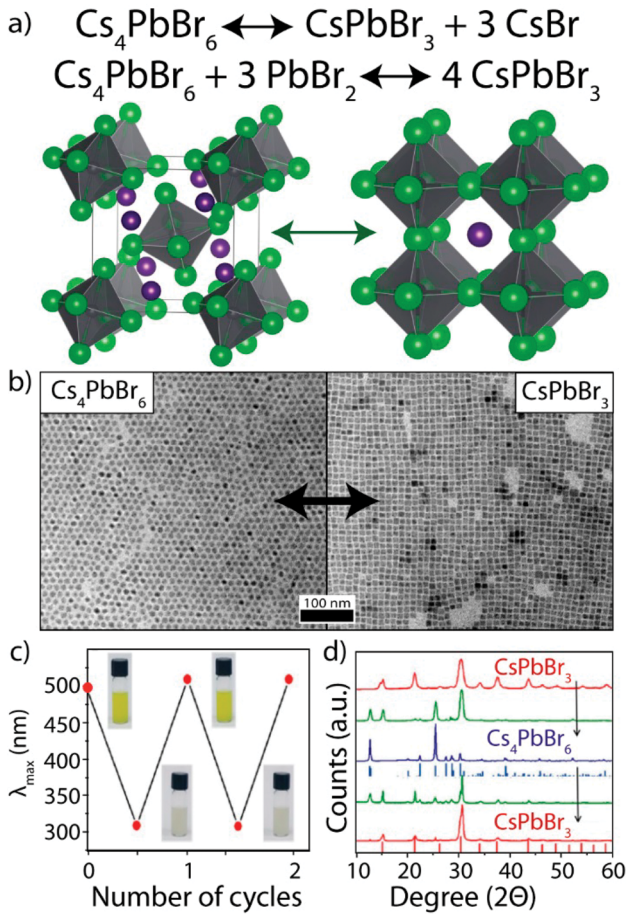

Figure 5. Overview of transformation reactions of Cs_4PbBr_6 into $CsPbBr_3$ and back. (a) Proposed reaction mechanisms for the exchange reaction via the extraction of CsBr or the insertion of $PbBr_2$. (b) TEM image showing the preservation of NC size from Cs_4PbBr_6 NCs to $CsPbBr_3$ NCs, adapted from ref 13. (c) First excitonic absorption peak and (d) XRD pattern of NCs after several reversible exchanges from $CsPbBr_3$ to Cs_4PbBr_6 and back, adapted from ref 37.

Due to the insulator bandgap and the very low conductive properties of Cs_4PbX_6 (either luminescent or nonluminescent), its widespread use in applications remains to be seen.

DOI: 10.1021/acs.jpclett.8b00572
J. Phys. Chem. Lett. 2018, 9, 2326−2337

AUTHOR INFORMATION

Corresponding Authors

*E-mail: ahmed.abdelhady@iit.it (A.L.A.).
*E-mail: liberato.manna@iit.it (L.M.).

ORCID

Ahmed L. Abdelhady: 0000-0002-6637-8853
Liberato Manna: 0000-0003-4386-7985

Notes

The authors declare no competing financial interest.

Biographies

Quinten Adriaan Akkerman is a Ph.D. student in the nanochemistry department at Istituto Italiano di Tecnologia (IIT), Genova, Italy. He obtained his bachelor's degree in Chemistry (2012) and master's degree in Chemistry and Physics (2014) at the University of Utrecht, Netherlands. Here, as part of his master thesis, he worked on the size, shape, and composition control of copper chalcogenide nanocrystals, under the supervision of Dr. Celso de Mello Donega. In 2015, he joined Liberato Manna's group as a Ph.D. student at IIT Genova, where he currently is focused on the development of novel synthesis methods and the characterization of perovskite and perovskite-related nanocrystals.

Ahmed L. Abdelhady holds a Ph.D. in inorganic chemistry from The University of Manchester, United Kingdom (2011), under the supervision of Prof. Paul O'Brien. After he completed his Ph.D., he became a lecturer of inorganic chemistry at Mansoura University, Egypt. In 2013, he joined Prof. Osman Bakr's Functional Nanomaterials Lab at King Abdullah University of Science and Technology (KAUST), Saudi Arabia. In 2016, he joined Prof. Liberato Manna's group at the Italian Institute of Technology (IIT) as a postdoctoral fellow and then as a researcher in 2017. His research is focused on all-inorganic and hybrid perovskite single crystals and thin films for optoelectronic applications.

Liberato Manna received his M.Sc. in Chemistry from the University of Bari (Italy) in 1996 and his Ph.D. in Chemical Sciences from the same University in 2001. During his Ph.D. studies and later as a postdoctoral fellow, he worked at the University of California Berkeley (U.S.A.). In 2003, he moved back to Italy as staff scientist at the National Nanotechnology Lab of CNR-INFM in Lecce (Italy) where he later became responsible for the Nanochemistry Division in 2006. In April 2009, he moved to the Istituto Italiano di Tecnologia in Genova as head of the Nanochemistry Department.

ACKNOWLEDGMENTS

The authors acknowledge financial support from the seventh European Community Framework Programme under Grant Agreement No. 614897 (ERC Consolidator Grant "TRANS-NANO"). We thank Urko Petralanda for providing Figure 1b.

REFERENCES

(1) Goldschmidt, V. M. Die Gesetze Der Krystallochemie. *Naturwissenschaften* **1926**, *14*, 477−485.
(2) Wells, H. L. Über Die Cäsium- Und Kalium-Bleihalogenide. *Z. anorg. allg. Chem.* **1893**, *3*, 195−210.
(3) Nikl, M.; Mihokova, E.; Nitsch, K. Photoluminescence & Decay Kinetics of Cs_4PbCl_6 Single Crystals. *Solid State Commun.* **1992**, *84*, 1089−1092.
(4) Nikl, M.; Nitsch, K.; Polak, K.; Pazzi, G. P.; Fabeni, P.; Citrin, D. S.; Gurioli, M. Optical-Properties of the Pb^{2+} Based Aggregated Phase in a CsCl Host Crystal − Quantum-Confinement Effects. *Phys. Rev. B: Condens. Matter Mater. Phys.* **1995**, *51*, 5192−5199.
(5) Nikl, M.; et al. Quantum Size Effect in the Excitonic Luminescence of $CsPbX_3$-Like Quantum Dots in CsX (X = Cl, Br) Single Crystal Host. *J. Lumin.* **1997**, *72-74*, 377−379.
(6) Nikl, M.; Mihokova, E.; Nitsch, K.; Somma, F.; Giampaolo, C.; Pazzi, G. P.; Fabeni, P.; Zazubovich, S. Photoluminescence of Cs_4PbBr_6 Crystals and Thin Films. *Chem. Phys. Lett.* **1999**, *306*, 280−284.
(7) Kondo, S.; Sakai, T.; Tanaka, H.; Saito, T. Amorphization-Induced Strong Localization of Electronic States in $CsPbBr_3$ and $CsPbCl_3$ Studied by Optical Absorption Measurements. *Phys. Rev. B: Condens. Matter Mater. Phys.* **1998**, *58*, 11401−11407.
(8) Kondo, S.; Amaya, K.; Higuchi, S.; Saito, T.; Asada, H.; Ishikane, M. Fundamental Optical Absorption of Cs_4PbCl_6. *Solid State Commun.* **2001**, *120*, 141−144.
(9) Kondo, S.; Masaki, A.; Saito, T.; Asada, H. Fundamental Optical Absorption of $CsPbI_3$ and Cs_4PbI_6. *Solid State Commun.* **2002**, *124*, 211−214.
(10) Perovskite Fever. *Nat. Mater.* **2014**, *13*, 837.10.1038/nmat4079
(11) Saidaminov, M. I.; et al. Pure Cs_4PbBr_6: Highly Luminescent Zero-Dimensional Perovskite Solids. *ACS Energy Lett.* **2016**, *1*, 840−845.
(12) Chen, D.; Wan, Z.; Chen, X.; Yuan, Y.; Zhong, J. Large-Scale Room-Temperature Synthesis and Optical Properties of Perovskite-Related Cs_4PbBr_6 Fluorophores. *J. Mater. Chem. C* **2016**, *4*, 10646−10653.
(13) Akkerman, Q. A.; et al. Nearly Monodisperse Insulator Cs_4PbX_6 (X = Cl, Br, I) Nanocrystals, Their Mixed Halide Compositions, and Their Transformation into $CsPbX_3$ Nanocrystals. *Nano Lett.* **2017**, *17*, 1924−1930.
(14) Zhang, Y.; et al. Zero-Dimensional Cs_4PbBr_6 Perovskite Nanocrystals. *J. Phys. Chem. Lett.* **2017**, *8*, 961−965.
(15) Protesescu, L.; Yakunin, S.; Bodnarchuk, M. I.; Krieg, F.; Caputo, R.; Hendon, C. H.; Yang, R. X.; Walsh, A.; Kovalenko, M. V. Nanocrystals of Cesium Lead Halide Perovskites ($CsPbX_3$, X = Cl, Br, and I): Novel Optoelectronic Materials Showing Bright Emission with Wide Color Gamut. *Nano Lett.* **2015**, *15*, 3692−3696.
(16) Bohun, A.; Dolejší, J.; Barta, Č. The Absorption and Luminescence of $(PbCl_6)^{4-}$ and $(PbBr_6)^{4-}$ Complexes. *Czech. J. Phys.* **1970**, *20*, 803−807.
(17) Yin, J.; Zhang, Y.; Bruno, A.; Soci, C.; Bakr, O. M.; Brédas, J.-L.; Mohammed, O. F. Intrinsic Lead Ion Emissions in Zero-Dimensional Cs_4PbBr_6 Nanocrystals. *ACS Energy Lett.* **2017**, *2*, 2805−2811.
(18) Zhang, H.; Liao, Q.; Wu, Y.; Chen, J.; Gao, Q.; Fu, H. Pure Zero-Dimensional Cs_4PbBr_6 Single Crystal Rhombohedral Microdisks with High Luminescence and Stability. *Phys. Chem. Chem. Phys.* **2017**, *19*, 29092−29098.
(19) Yin, J.; Maity, P.; De Bastiani, M.; Dursun, I.; Bakr, O. M.; Brédas, J.-L.; Mohammed, O. F. Molecular Behavior of Zero-Dimensional Perovskites. *Sci. Adv.* **2017**, *3*, e1701793.
(20) Seth, S.; Samanta, A. Fluorescent Phase-Pure Zero-Dimensional Perovskite-Related Cs_4PbBr_6 Microdisks: Synthesis and Single-Particle Imaging Study. *J. Phys. Chem. Lett.* **2017**, *8*, 4461−4467.
(21) De Bastiani, M.; et al. Inside Perovskites: Quantum Luminescence from Bulk Cs_4PbBr_6 Single Crystals. *Chem. Mater.* **2017**, *29*, 7108−7113.
(22) Yang, H.; Zhang, Y.; Pan, J.; Yin, J.; Bakr, O. M.; Mohammed, O. F.; et al. Room-Temperature Engineering of All-Inorganic Perovskite Nanocrsytals with Different Dimensionalities. *Chem. Mater.* **2017**, *29*, 8978−8982.
(23) Seth, S.; Samanta, A. Photoluminescence of Zero-Dimensional Perovskites and Perovskite-Related Materials. *J. Phys. Chem. Lett.* **2018**, *9*, 176−183.
(24) Saidaminov, M. I.; Mohammed, O. F.; Bakr, O. M. Low-Dimensional-Networked Metal Halide Perovskites: The Next Big Thing. *ACS Energy Lett.* **2017**, *2*, 889−896.
(25) Pal, P.; Saha, S.; Banik, A.; Sarkar, A.; Biswas, K. All-Solid-State Mechanochemical Synthesis and Post-Synthetic Transformation of Inorganic Perovskite-Type Halides. *Chem. - Eur. J.* **2018**, *24*, 1811−1815.

DOI: 10.1021/acs.jpclett.8b00572
J. Phys. Chem. Lett. 2018, 9, 2326−2337

(26) Zhang, Y.; Sinatra, L.; Alarousu, E.; Yin, J.; El-Zohry, A. M.; Bakr, O. M.; Mohammed, O. F. Ligand-Free Nanocrystals of Highly Emissive Cs_4PbBr_6 Perovskite. *J. Phys. Chem. C* **2018**, *122*, 6493.
(27) Wu, L.; et al. From Nonluminescent Cs_4PbX_6 (X = Cl, Br, I) Nanocrystals to Highly Luminescent $CsPbX_3$ Nanocrystals: Water-Triggered Transformation through a CsX-Stripping Mechanism. *Nano Lett.* **2017**, *17*, 5799−5804.
(28) Palazon, F.; et al. Postsynthesis Transformation of Insulating Cs_4PbBr_6 Nanocrystals into Bright Perovskite $CsPbBr_3$ through Physical and Chemical Extraction of CsBr. *ACS Energy Lett.* **2017**, *2*, 2445−2448.
(29) Hu, M.; Ge, C.; Yu, J.; Feng, J. Mechanical and Optical Properties of Cs_4BX_6 (B = Pb, Sn; X = Cl, Br, I) Zero-Dimension Perovskites. *J. Phys. Chem. C* **2017**, *121*, 27053−27058.
(30) Xu, J.; et al. Imbedded Nanocrystals of $CsPbBr_3$ in Cs_4PbBr_6: Kinetics, Enhanced Oscillator Strength, and Application in Light-Emitting Diodes. *Adv. Mater.* **2017**, *29*, 1703703.
(31) de Weerd, C.; Lin, J.; Gomez, L.; Fujiwara, Y.; Suenaga, K.; Gregorkiewicz, T. Hybridization of Single Nanocrystals of Cs_4PbBr_6 and $CsPbBr_3$. *J. Phys. Chem. C* **2017**, *121*, 19490−19496.
(32) Wang, Y.; Yu, D.; Wang, Z.; Li, X.; Chen, X.; Nalla, V.; Zeng, H.; Sun, H. Solution-Grown $CsPbBr_3/Cs_4PbBr_6$ Perovskite Nanocomposites: Toward Temperature-Insensitive Optical Gain. *Small* **2017**, *13*, 1701587.
(33) Liu, Z.; et al. Ligand Mediated Transformation of Cesium Lead Bromide Perovskite Nanocrystals to Lead Depleted Cs_4PbBr_6 Nanocrystals. *J. Am. Chem. Soc.* **2017**, *139*, 5309−5312.
(34) Chen, X. Centimeter-Sized Cs_4PbBr_6 Crystals with Embedded $CsPbBr_3$ Nanocrystals Showing Superior Photoluminescence: Nonstoichiometry Induced Transformation and Light-Emitting Applications. *Adv. Funct. Mater.* **2018**, 1706567.
(35) Yang, L.; Li, D.; Wang, C.; Yao, W.; Wang, H.; Huang, K. Room-Temperature Synthesis of Pure Perovskite-Related Cs4PbBr$_6$ Nanocrystals and Their Ligand-Mediated Evolution into Highly Luminescent $CsPbBr_3$ Nanosheets. *J. Nanopart. Res.* **2017**, *19*, 258.
(36) Hu, H.; et al. Interfacial Synthesis of Highly Stable $CsPbX_3$/Oxide Janus Nanoparticles. *J. Am. Chem. Soc.* **2018**, *140*, 406−412.
(37) Udayabhaskararao, T.; et al. A Mechanistic Study of Phase Transformation in Perovskite Nanocrystals Driven by Ligand Passivation. *Chem. Mater.* **2018**, *30*, 84−93.
(38) Xu, L.; et al. Double-Protected All-Inorganic Perovskite Nanocrystals by Crystalline Matrix and Silica for Triple-Modal Anti-Counterfeiting Codes. *ACS Appl. Mater. Interfaces* **2017**, *9*, 26556−26564.
(39) Palazon, F.; Almeida, G.; Akkerman, Q. A.; De Trizio, L.; Dang, Z.; Prato, M.; Manna, L. Changing the Dimensionality of Cesium Lead Bromide Nanocrystals by Reversible Postsynthesis Transformations with Amines. *Chem. Mater.* **2017**, *29*, 4167−4171.
(40) Ling, Y.; Tan, L.; Wang, X.; Zhou, Y.; Xin, Y.; Ma, B.; Hanson, K.; Gao, H. Composite Perovskites of Cesium Lead Bromide for Optimized Photoluminescence. *J. Phys. Chem. Lett.* **2017**, *8*, 3266−3271.
(41) Kang, B.; Biswas, K. Exploring Polaronic, Excitonic Structures and Luminescence in $Cs_4PbBr_6/CsPbBr_3$. *J. Phys. Chem. Lett.* **2018**, *9*, 830−836.
(42) Tong, G.; Li, H.; Zhu, Z.; Zhang, Y.; Yu, L.; Xu, J.; Jiang, Y. Enhancing Hybrid Perovskite Detectability in Deep Ultraviolet Region with Down-Conversion Dual-Phase ($CsPbBr_3$−Cs_4PbBr_6) Films. *J. Phys. Chem. Lett.* **2018**, *9*, 1592.
(43) Akkerman, Q. A. Genesis, Challenges and Opportunities for Colloidal Lead Halide Perovskite Nanocrystals. *Nat. Mater.* **2018**, DOI: 10.1038/s41563-018-0018-4.
(44) Bergerhoff, G.; Schmitz-Dumont, O. Die Struktur Von Kaliumcadmiumchlorid K_4CdCl_6. *Naturwissenschaften* **1954**, *41*, 280−281.
(45) Beck, H. P.; Milius, W. Study on A_4BX_6 Compounds. I. Structure Refinement of Ternary Cd Halides A_4CdX_6 (A = NH_4, K, Rb, In, Tl; X = Cl, I). *Z. Anorg. Allg. Chem.* **1986**, *539*, 7−17.
(46) Komer, W. D.; Machin, D. J. Ternary and Quaternary Oxides of Ruthenium and Iridium. *J. Less-Common Met.* **1978**, *61*, 91−105.
(47) Sun, Q.; Qu, B.; Shi, J. Investigation of Relations between Absorption Band Positions and Crystalline Environment in Pb^{2+}-Doped Alkali Halides. *Phys. Chem. Chem. Phys.* **2010**, *12*, 4178−4183.
(48) Aceves, R.; et al. Relaxed Excited States Origin and Structure in Lead-Doped Caesium Bromide. *Phys. Status Solidi B* **2001**, *223*, 745−756.
(49) Ahmad, W.; Khan, J.; Niu, G.; Tang, J. Inorganic $CsPbI_3$ Perovskite-Based Solar Cells: A Choice for a Tandem Device. *Solar RRL* **2017**, *1*, 1700048.
(50) Ma, F.; Li, J.; Li, W.; Lin, N.; Wang, L.; Qiao, J. Stable a/d Phase Junction of Formamidinium Lead Iodide Perovskites for Enhanced near-Infrared Emission. *Chem. Sci.* **2017**, *8*, 800−805.
(51) Cao, D. H.; Stoumpos, C. C.; Farha, O. K.; Hupp, J. T.; Kanatzidis, M. G. 2D Homologous Perovskites as Light-Absorbing Materials for Solar Cell Applications. *J. Am. Chem. Soc.* **2015**, *137*, 7843−7850.
(52) Dursun, I.; et al. $CsPb_2Br_5$ Single Crystals: Synthesis and Characterization. *ChemSusChem* **2017**, *10*, 3746−3749.
(53) Cha, J.-H.; Han, J. H.; Yin, W.; Park, C.; Park, Y.; Ahn, T. K.; Cho, J. H.; Jung, D.-Y. Photoresponse of $CsPbBr_3$ and Cs_4PbBr_6 Perovskite Single Crystals. *J. Phys. Chem. Lett.* **2017**, *8*, 565−570.
(54) Rakita, Y.; et al. Low-Temperature Solution-Grown $CsPbBr_3$ Single Crystals and Their Characterization. *Cryst. Growth Des.* **2016**, *16*, 5717−5725.
(55) Nikl, M.; et al. Luminescence of $CsPbBr_3$-Like Quantum Dots in CsBr Single Crystals. *Phys. E* **1999**, *4*, 323−331.
(56) Aceves, R.; et al. Spectroscopy of $CsPbBr_3$ Quantum Dots in CsBr:Pb Crystals. *J. Lumin.* **2001**, *93*, 27−41.
(57) Kondo, S.-I.; Kakuchi, M.; Masaki, A.; Saito, T. Strongly Enhanced Free-Exciton Luminescence in Microcrystalline $CsPbBr_3$ Films. *J. Phys. Soc. Jpn.* **2003**, *72*, 1789−1791.
(58) Kondo, S.; Nakagawa, H.; Saito, T.; Asada, H. Extremely Photo-Luminescent Microcrystalline $CsPbX_3$ (X = Cl, Br) Films Obtained by Amorphous-to-Crystalline Transformation. *Curr. Appl. Phys.* **2004**, *4*, 439−444.
(59) Kondo, S.; Saito, T.; Asada, H.; Nakagawa, H. Stimulated Emission from Microcrystalline $CsPbBr_3$ Films: Edge Emission Versus Surface Emission. *Mater. Sci. Eng., B* **2007**, *137*, 156−161.
(60) Kondo, S.; Takahashi, K.; Nakanish, T.; Saito, T.; Asada, H.; Nakagawa, H. High Intensity Photoluminescence of Microcrystalline $CsPbBr_3$ Films: Evidence for Enhanced Stimulated Emission at Room Temperature. *Curr. Appl. Phys.* **2007**, *7*, 1−5.
(61) Lee, J.-W.; et al. In-Situ Formed Type I Nanocrystalline Perovskite Film for Highly Efficient Light-Emitting Diode. *ACS Nano* **2017**, *11*, 3311−3319.
(62) Quan, L. N.; Quintero-Bermudez, R.; Voznyy, O.; Walters, G.; Jain, A.; Fan, J. Z.; Zheng, X.; Yang, Z.; Sargent, E. H. Highly Emissive Green Perovskite Nanocrystals in a Solid State Crystalline Matrix. *Adv. Mater.* **2017**, *29*, 1605945.
(63) Srimath Kandada, A. R.; et al. Nonlinear Carrier Interactions in Lead Halide Perovskites and the Role of Defects. *J. Am. Chem. Soc.* **2016**, *138*, 13604−13611.
(64) Motti, S. G.; Gandini, M.; Barker, A. J.; Ball, J. M.; Srimath Kandada, A. R.; Petrozza, A. Photoinduced Emissive Trap States in Lead Halide Perovskite Semiconductors. *ACS Energy Lett.* **2016**, *1*, 726−730.
(65) Shi, H.; Du, M.-H. Shallow Halogen Vacancies in Halide Optoelectronic Materials. *Phys. Rev. B: Condens. Matter Mater. Phys.* **2014**, *90*, 174103.
(66) Steirer, K. X.; Schulz, P.; Teeter, G.; Stevanovic, V.; Yang, M.; Zhu, K.; Berry, J. J. Defect Tolerance in Methylammonium Lead Triiodide Perovskite. *ACS Energy Lett.* **2016**, *1*, 360−366.
(67) Kang, J.; Wang, L.-W. High Defect Tolerance in Lead Halide Perovskite $CsPbBr_3$. *J. Phys. Chem. Lett.* **2017**, *8*, 489−493.
(68) Huang, H.; Bodnarchuk, M.; Kershaw, S. V.; Kovalenko, M. V.; Rogach, A. L. Lead Halide Perovskite Nanocrystals in the Research

DOI: 10.1021/acs.jpclett.8b00572
J. Phys. Chem. Lett. 2018, 9, 2326−2337

Spotlight: Stability and Defect-Tolerance. *ACS Energy Lett.* **2017**, *2*, 2071−2083.
(69) Kovalenko, M. V.; Protesescu, L.; Bodnarchuk, M. I. Properties and Potential Optoelectronic Applications of Lead Halide Perovskite Nanocrystals. *Science* **2017**, *358*, 745−750.
(70) Yuan, Y.; Chae, J.; Shao, Y.; Wang, Q.; Xiao, Z.; Centrone, A.; Huang, J. Photovoltaic Switching Mechanism in Lateral Structure Hybrid Perovskite Solar Cells. *Adv. Energy Mater.* **2015**, *5*, 1500615.
(71) Shi, T.; Yin, W.-J.; Hong, F.; Zhu, K.; Yan, Y. Unipolar Self-Doping Behavior in Perovskite $CH_3NH_3PbBr_3$. *Appl. Phys. Lett.* **2015**, *106*, 103902.
(72) Buin, A.; Comin, R.; Xu, J.; Ip, A. H.; Sargent, E. H. Halide-Dependent Electronic Structure of Organolead Perovskite Materials. *Chem. Mater.* **2015**, *27*, 4405−4412.
(73) Kim, J.; Lee, S.-H.; Lee, J. H.; Hong, K.-H. The Role of Intrinsic Defects in Methylammonium Lead Iodide Perovskite. *J. Phys. Chem. Lett.* **2014**, *5*, 1312−1317.
(74) Buin, A.; Pietsch, P.; Xu, J.; Voznyy, O.; Ip, A. H.; Comin, R.; Sargent, E. H. Materials Processing Routes to Trap-Free Halide Perovskites. *Nano Lett.* **2014**, *14*, 6281−6286.
(75) Luo, Y.; Khoram, P.; Brittman, S.; Zhu, Z.; Lai, B.; Ong, S. P.; Garnett, E. C.; Fenning, D. P. Direct Observation of Halide Migration and Its Effect on the Photoluminescence of Methylammonium Lead Bromide Perovskite Single Crystals. *Adv. Mater.* **2017**, *29*, 1703451.
(76) Yantara, N.; Bhaumik, S.; Yan, F.; Sabba, D.; Dewi, H. A.; Mathews, N.; Boix, P. P.; Demir, H. V.; Mhaisalkar, S. Inorganic Halide Perovskites for Efficient Light-Emitting Diodes. *J. Phys. Chem. Lett.* **2015**, *6*, 4360−4364.
(77) Xiao, Z.; Yan, Y.; Hosono, H.; Kamiya, T. Roles of Pseudo-Closed S2 Orbitals for Different Intrinsic Hole Generation between Tl−Bi and In−Bi Bromide Double Perovskites. *J. Phys. Chem. Lett.* **2018**, *9*, 258−262.
(78) Xu, J.; Liu, J.-B.; Liu, B.-X.; Huang, B. Intrinsic Defect Physics in Indium-Based Lead-Free Halide Double Perovskites. *J. Phys. Chem. Lett.* **2017**, *8*, 4391−4396.
(79) Seth, S.; Mondal, N.; Patra, S.; Samanta, A. Fluorescence Blinking and Photoactivation of All-Inorganic Perovskite Nanocrystals $CsPbBr_3$ and $CsPbBr_2I$. *J. Phys. Chem. Lett.* **2016**, *7*, 266−271.
(80) Cho, H.; et al. Overcoming the Electroluminescence Efficiency Limitations of Perovskite Light-Emitting Diodes. *Science* **2015**, *350*, 1222−1225.
(81) Komesu, T.; et al. Surface Electronic Structure of Hybrid Organo Lead Bromide Perovskite Single Crystals. *J. Phys. Chem. C* **2016**, *120*, 21710−21715.
(82) Imran, M.; Caligiuri, V.; Wang, M.; Goldoni, L.; Prato, M.; Krahne, R.; De Trizio, L.; Manna, L. Benzoyl Halides as Alternative Precursors for the Colloidal Synthesis of Lead-Based Halide Perovskite Nanocrystals. *J. Am. Chem. Soc.* **2018**, *140*, 2656.
(83) Woo, J. Y.; Kim, Y.; Bae, J.; Kim, T. G.; Kim, J. W.; Lee, D. C.; Jeong, S. Highly Stable Cesium Lead Halide Perovskite Nanocrystals through in Situ Lead Halide Inorganic Passivation. *Chem. Mater.* **2017**, *29*, 7088−7092.
(84) Dohner, E. R.; Jaffe, A.; Bradshaw, L. R.; Karunadasa, H. I. Intrinsic White-Light Emission from Layered Hybrid Perovskites. *J. Am. Chem. Soc.* **2014**, *136*, 13154−13157.
(85) Yuan, Z.; et al. One-Dimensional Organic Lead Halide Perovskites with Efficient Bluish White-Light Emission. *Nat. Commun.* **2017**, *8*, 14051.
(86) Zhou, C.; et al. Highly Efficient Broadband Yellow Phosphor Based on Zero-Dimensional Tin Mixed-Halide Perovskite. *ACS Appl. Mater. Interfaces* **2017**, *9*, 44579−44583.
(87) Zhou, C.; et al. Luminescent Zero-Dimensional Organic Metal Halide Hybrids with near-Unity Quantum Efficiency. *Chem. Sci.* **2018**, *9*, 586−593.
(88) Akkerman, Q. A.; D'Innocenzo, V.; Accornero, S.; Scarpellini, A.; Petrozza, A.; Prato, M.; Manna, L. Tuning the Optical Properties of Cesium Lead Halide Perovskite Nanocrystals by Anion Exchange Reactions. *J. Am. Chem. Soc.* **2015**, *137*, 10276−10281.
(89) Talapin, D. V.; Lee, J.-S.; Kovalenko, M. V.; Shevchenko, E. V. Prospects of Colloidal Nanocrystals for Electronic and Optoelectronic Applications. *Chem. Rev.* **2010**, *110*, 389−458.
(90) Song, Y. H.; et al. Innovatively Continuous Mass Production Couette-Taylor Flow: Pure Inorganic Green-Emitting Cs_4PbBr_6 Perovskite Microcrystal for Display Technology. *Sci. Rep.* **2018**, *8*, 2009.
(91) Yuan, Z.; Zhou, C.; Messier, J.; Tian, Y.; Shu, Y.; Wang, J.; Xin, Y.; Ma, B. A Microscale Perovskite as Single Component Broadband Phosphor for Downconversion White-Light-Emitting Devices. *Adv. Opt. Mater.* **2016**, *4*, 2009−2015.
(92) Lin, H.; Zhou, C.; Tian, Y.; Siegrist, T.; Ma, B. Low-Dimensional Organometal Halide Perovskites. *ACS Energy Lett.* **2018**, *3*, 54−62.
(93) Zhou, C.; et al. Low-Dimensional Organic Tin Bromide Perovskites and Their Photoinduced Structural Transformation. *Angew. Chem.* **2017**, *129*, 9146−9150.
(94) Smith, M. D.; Jaffe, A.; Dohner, E. R.; Lindenberg, A. M.; Karunadasa, H. I. Structural Origins of Broadband Emission from Layered Pb-Br Hybrid Perovskites. *Chem. Sci.* **2017**, *8*, 4497−4504.
(95) Baker, D. R.; Kamat, P. V. Tuning the Emission of CdSe Quantum Dots by Controlled Trap Enhancement. *Langmuir* **2010**, *26*, 11272−11276.
(96) Sahu, A.; Kang, M. S.; Kompch, A.; Notthoff, C.; Wills, A. W.; Deng, D.; Winterer, M.; Frisbie, C. D.; Norris, D. J. Electronic Impurity Doping in CdSe Nanocrystals. *Nano Lett.* **2012**, *12*, 2587−2594.
(97) Castro, S. L.; Bailey, S. G.; Raffaelle, R. P.; Banger, K. K.; Hepp, A. F. Synthesis and Characterization of Colloidal $Cuins_2$ Nanoparticles from a Molecular Single-Source Precursor. *J. Phys. Chem. B* **2004**, *108*, 12429−12435.
(98) Hu, T.; et al. Mechanism for Broadband White-Light Emission from Two-Dimensional (110) Hybrid Perovskites. *J. Phys. Chem. Lett.* **2016**, *7*, 2258−2263.
(99) Wu, K.; Liang, G.; Shang, Q.; Ren, Y.; Kong, D.; Lian, T. Ultrafast Interfacial Electron and Hole Transfer from $CsPbBr_3$ Perovskite Quantum Dots. *J. Am. Chem. Soc.* **2015**, *137*, 12792−12795.
(100) Liu, F.; et al. Highly Luminescent Phase-Stable $CsPbI_3$ Perovskite Quantum Dots Achieving near 100% Absolute Photoluminescence Quantum Yield. *ACS Nano* **2017**, *11*, 10373−10383.
(101) Liu, S.; He, M.; Di, X.; Li, P.; Xiang, W.; Liang, X. Precipitation and Tunable Emission of Cesium Lead Halide Perovskites ($CsPbX_3$, X = Br, I) QDs in Borosilicate Glass. *Ceram. Int.* **2018**, *44*, 4496−4499.
(102) Almeida, G.; Goldoni, L.; Akkerman, Q.; Dang, Z.; Khan, A. H.; Marras, S.; Moreels, I.; Manna, L. Role of Acid-Base Equilibria in the Size, Shape, and Phase Control of Cesium Lead Bromide Nanocrystals. *ACS Nano* **2018**, *12*, 1704.
(103) Zhang, Z.; Zhu, Y.; Wang, W.; Zheng, W.; Lin, R.; Huang, F. Growth, Characterization and Optoelectronic Applications of Pure-Phase Large-Area $CsPb_2Br_5$ Flake Single Crystals. *J. Mater. Chem. C* **2018**, *6*, 446−451.
(104) Li, G.; Wang, H.; Zhu, Z.; Chang, Y.; Zhang, T.; Song, Z.; Jiang, Y. Shape and Phase Evolution from $CsPbBr_3$ Perovskite Nanocubes to Tetragonal $CsPb_2Br_5$ Nanosheets with an Indirect Bandgap. *Chem. Commun.* **2016**, *52*, 11296−11299.
(105) Li, J.; et al. Synthesis of All-Inorganic $CsPb_2Br_5$ Perovskite and Determination of Its Luminescence Mechanism. *RSC Adv.* **2017**, *7*, 54002−54007.
(106) Qin, C.; Matsushima, T.; Sandanayaka, A. S. D.; Tsuchiya, Y.; Adachi, C. Centrifugal-Coated Quasi-Two-Dimensional Perovskite $CsPb_2Br_5$ Films for Efficient and Stable Light-Emitting Diodes. *J. Phys. Chem. Lett.* **2017**, *8*, 5415−5421.
(107) Lv, J.; Fang, L.; Shen, J. Synthesis of Highly Luminescent $CsPb_2Br_5$ Nanoplatelets and Their Application for Light-Emitting Diodes. *Mater. Lett.* **2018**, *211*, 199−202.
(108) Balakrishnan, S. K.; Kamat, P. V. Ligand Assisted Transformation of Cubic $CsPbBr_3$ Nanocrystals into Two-Dimensional $CsPb_2Br_5$ Nanosheets. *Chem. Mater.* **2018**, *30*, 74−78.

DOI: 10.1021/acs.jpclett.8b00572
J. Phys. Chem. Lett. 2018, 9, 2326−2337

(109) Ruan, L.; Shen, W.; Wang, A.; Xiang, A.; Deng, Z. Alkyl-Thiol Ligand-Induced Shape- and Crystalline Phase-Controlled Synthesis of Stable Perovskite-Related $CsPb_2Br_5$ Nanocrystals at Room Temperature. *J. Phys. Chem. Lett.* **2017**, *8*, 3853−3860.
(110) Moller, C. K. Crystal Structure and Photoconductivity of Caesium Plumbohalides. *Nature* **1958**, *182*, 1436−1436.
(111) Andrews, R. H.; Clark, S. J.; Donaldson, J. D.; Dewan, J. C.; Silver, J. Solid-State Properties of Materials of the Type Cs_4MX_6 (Where M = Sn or Pb and X = Cl or Br). *J. Chem. Soc., Dalton Trans.* **1983**, 767−770.
(112) Babin, V.; Fabeni, P.; Nikl, M.; Pazzi, G. P.; Sildos, I.; Zazubovich, N.; Zazubovich, S. Polarized Luminescence of $CsPbBr_3$ Nanocrystals (Quantum Dots) in CsBr:Pb Single Crystal. *Chem. Phys. Lett.* **1999**, *314*, 31−36.
(113) Guhrenz, C.; Benad, A.; Ziegler, C.; Haubold, D.; Gaponik, N.; Eychmüller, A. Solid-State Anion Exchange Reactions for Color Tuning of $CsPbX_3$ Perovskite Nanocrystals. *Chem. Mater.* **2016**, *28*, 9033−9040.
(114) Shamsi, J.; Dang, Z.; Ijaz, P.; Abdelhady, A. L.; Bertoni, G.; Moreels, I.; Manna, L. Colloidal CsX (X = Cl, Br, I) Nanocrystals and Their Transformation to $CsPbX_3$ Nanocrystals by Cation Exchange. *Chem. Mater.* **2018**, *30*, 79−83.

DOI: 10.1021/acs.jpclett.8b00572
J. Phys. Chem. Lett. 2018, 9, 2326−2337